Highlighting joint research results from International Center for Synchrotron Radiation Innovation Smart (SRIS), Tohoku University, DENSO CORPORATION, and Japan Synchrotron Radiation Research Institute/SPring-8.

Dynamic behaviours of epoxy resin thin films during the curing process

Capillary waves during the curing process of epoxy resin thin films were investigated using grazing incidence X-ray photon correlation spectroscopy. The freezing behaviour during the curing reaction was successfully observed.

As featured in:

See Taiki Hoshino *et al.*,
Soft Matter, 2023, **19**, 3267.

ROYAL SOCIETY
OF **CHEMISTRY**

rsc.li/soft-matter-journal

Dynamic behaviours of epoxy resin thin films during the curing process†

Taiki Hoshino, [ID] *[abc] Yasushi Okamoto,[d] Atsushi Yamamoto[d] and Hiroyasu Masunaga[e]

Epoxy resin thin films are widely used in applications such as coating materials, insulator films, and adhesives; accordingly, investigations of their physical properties have garnered increasing importance. Although the physical properties of thermoset epoxy thin films are strongly affected by the curing conditions, such as the heating temperature and curing time, the dynamic properties during the curing process have not been studied thoroughly. In this study, we investigated the thermal fluctuations on the surface of epoxy resin thin films using grazing-incidence X-ray photon correlation spectroscopy, to elucidate the dynamic behaviours during the curing process. We thus succeeded in observing the freezing of capillary waves during the thermal curing process. These results are expected to facilitate a deeper understanding of the curing mechanisms of various thin films.

1 Introduction

Epoxy resins are essential materials for modern industry because of their excellent mechanical properties, chemical resistance, and moldability.[1,2] The physical properties of epoxy products are considerably affected by the curing process;[3] therefore, various studies have been conducted on the curing mechanisms and variation of physical properties during the curing process. To elucidate the reaction mechanisms, the reaction kinetics have been analyzed using various techniques, such as differential scanning calorimetry,[4–6] near-infrared spectroscopy and Raman spectroscopy.[4,7,8] The kinetics of the mechanical properties have been examined using rheological methods.[9–12] Mathematical models and computer simulations of various chemical reactions have been employed to investigate the details of the curing reaction process and its correlation with the macroscopic properties.[13–15] From the perspective of dynamic analysis, X-ray photon correlation spectroscopy (XPCS) studies have been also conducted.[16–18]

In addition to bulk systems, epoxy resins have been widely used in thin film structures, such as coatings, insulator films, and adhesives. Thus, the physical properties of epoxy-resin thin films, such as electrical insulation,[19] mechanical properties in composite materials,[20,21] and chemical state at substrate interface,[22–25] have attracted considerable interest and have been vigorously investigated. However, up to our knowledge, no studies have investigated dynamic surface fluctuations during the curing process of epoxy thin films.

In this study, we focus on capillary waves generated by the thermal fluctuations of molecules on fluid surfaces. The surface of a fluid in equilibrium is macroscopically smooth; however, microscopic surface fluctuations occur due to the molecular motion. The dynamical behaviour of surface fluctuations is described in relation with the surface tension, viscosity, viscoelasticity, and thickness. The dynamics of capillary waves has been experimentally studied using coherent surface scattering techniques, namely, light scattering spectroscopy (LSS)[26–29] and grazing incidence X-ray photon correlation spectroscopy (GI-XPCS),[30,31] whereby the capillary wave spectra with scattering wave vector dependence and dynamic properties are obtained. In this study, the dynamics of capillary waves during the thermal curing of spin-coated thin films of diamine-based epoxy resin were investigated. This is the first report to observe the capillary wave dynamics under non-equilibrium conditions in a curing system. It can provide valuable insights into the fundamental study of non-equilibrium dynamics in low-dimensional systems.

2 Experimental

For an epoxy resin sample, we used bisphenol A diglycidyl ether (DGEBA) as the main ingredient and diaminodiphenylmethane

*a International Center for Synchrotron Radiation Innovation Smart (SRIS), Tohoku University, 2-1-1 Katahira, Aoba-ku, Sendai 980-8577, Japan.
E-mail: taiki.hoshino.c7@tohoku.ac.jp*

b Institute of Multidisciplinary Research for Advanced Materials (IMRAM), Tohoku University, 2-1-1 Katahira, Aoba-ku, Sendai 980-8577, Japan

c RIKEN SPring-8 Center, 1-1-1, Kouto, Sayo-cho, Sayo-gun, Hyogo 679-5148, Japan

d DENSO CORPORATION, 1-1, Showa-cho, Kariya, Aichi 448-8661, Japan

e Japan Synchrotron Radiation Research Institute/SPring-8, 1-1-1, Kouto, Sayo-cho, Sayo-gun, Hyogo 679-5198, Japan
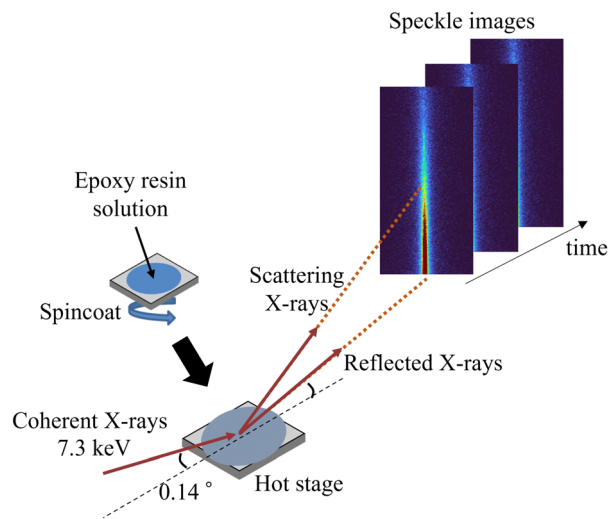
Fig. 1 Schematic illustration of GI-XPCS measurement in the curing process of the epoxy resin thin film.

(DDM) as the hardener. A mixture of DGEBA and DDM was dissolved in cyclopentanone, and spin-coated thin films were deposited on a silicon substrate. The film thickness was 370 nm, measured by an interferometer (Optical NanoGauge C11627, Hamamatsu Photonics).

The GI-XPCS measurements were performed at two different temperatures, 70 and 80 °C, to better interpret the observed data through discussing the temperature dependence. The GI-XPCS measurements were performed at beamline BL03XU of SPring-8,[32] as shown schematically in Fig. 1. The thin films were placed on a hot stage maintained at 70 or 80 °C in vacuum. After 240 s for the alignment, the samples were irradiated with highly coherent X-rays, obtained from a 7.3 keV X-ray beam passing through a 20 μm-diameter pinhole. The irradiation incidence angle was set at 0.14°, which was smaller than the total reflection critical angle. In this condition the penetration depth of the X-rays was estimated to be about 10 nm. Scattered X-rays were detected using an EIGER 1M two-dimensional detector (Dectris, Switzerland) mounted approximately 4 m downstream from the sample. With an exposure time of 0.3 s per frame, 1000 frames of scattering images were acquired every 3 s. Microscopic morphological observation showed that no damage was observed before or after irradiation, and no change in the scattering profiles due to the irradiation were observed (Fig. S1, ESI†).

The viscoelastic properties of the bulk sample were measured by the parallel plate rheometry using a Malvern KINEXUS lab+ (Malvern Panalytical, UK) with sinusoidal deformations at an amplitude of 0.1% and a frequency of 1 Hz. The sample was prepared by dissolving a mixture of DGEBA and DDM in cyclopentanone and evaporating the solvent in a vacuum.

3 Results and discussion

The capillary waves generated by thermal motion of molecules travel parallel to the surface, and their dynamics can be discussed by evaluating the fluctuations of the scattered speckles obtained by the diffuse scattering from the surface. From the scattering images obtained from the GI-XPCS measurements (Fig. S2a, ESI†), the following two-time correlation function was calculated

$$C_I(q_\parallel, t_1, t_2) = \frac{\langle I_p(q_\parallel, t_1) I_p(q_\parallel, t_2) \rangle_\Psi}{\langle I_p(q_\parallel, t_1) \rangle_\Psi \langle I_p(q_\parallel, t_2) \rangle_\Psi} \quad (1)$$

where $I_p(q_\parallel, t)$ is the detected intensity at $q_\parallel$, which is the in-plane component of the scattered wave vector, and time t, and $\langle \cdots \rangle_\Psi$ denotes the time-averaging over all pixels within $q_\parallel \pm \Delta q_\parallel$.[33,34] $\Delta q_\parallel$ was 2.5×10^{-4} nm^{-1} in this study (two-dimensional profile of $q_\parallel$ is shown in Fig. S2b, ESI†). Fig. 2a and b show C_I for $q_\parallel = 1.78 \times 10^{-3}$ nm^{-1} as representative observations at 70 and 80 °C, respectively. In the two-time correlation function, the temporal variation of the time autocorrelation function of the scattering intensity can be plotted visually, and the correlation function at a certain time can be evaluated by cutting out horizontally as shown by the white arrow in the Fig. 2a.[35] From the diagonal colour change, the change of relaxation time can be evaluated. Note that the origin of the time axis in Fig. 2 was set at 240 s, because the measurements started 240 s after the sample was placed.

In the 70 °C-curing process, in the initial stage, the diagonal colour change is hardly visible until around 1700 s as shown in Fig. 2a. This is because the surface fluctuations were too fast to show up as a clear colour change in C_I. After 1700 s, a slowdown is clearly observed. Although the diagonal band continuously thickens between 1700 and 2320 s, discontinuous colour change appears at around 2320 s (arrow A) and 2540 s (arrow B). The former represents continuous slowdown, while the latter represents increase of the base value. Similar changes are observed in the 80 °C-curing process but they occur faster than in the 70 °C-process. A clear slowdown occurs after 1200 s, and discontinuous increases of base value appear at around 1620 (arrow C) and 1890 s (arrow D).

For a more detailed analysis, the time autocorrelation function $g_2(q, \tau)$ was derived from C_I and analyzed, where $\tau = t_1 - t_2$. Fig. 3a and b show g_2 at various time t_w cuts from C_I for $q_\parallel = 1.78 \times 10^{-3}$ nm^{-1} at 70 and 80 °C, respectively. In all cases, g_2 was averaged over 10 data points when cut from C_I. At both 70 and 80 °C, the relaxations slowed down and the baseline increased with the elapsed time t_w. All g_2 were well represented by the following exponential function

$$g_2(q, \tau) = A \exp(-2\Gamma\tau) + \text{baseline} \quad (2)$$

where A is the constant value for time, and Γ is the relaxation rate. Here, if all the surface fluctuations are represented by the first term, A should be the speckle contrast determined by the experimental setup and the baseline should be 1. However, if there are other fluctuations longer than the measurement time, baseline should be larger than 1, and $A +$ baseline should be the speckle contrast.

Fig. 3c and d show the t_w dependence of Γ and baseline at 70 and 80 °C obtained by fitting analysis with eqn (2), respectively.
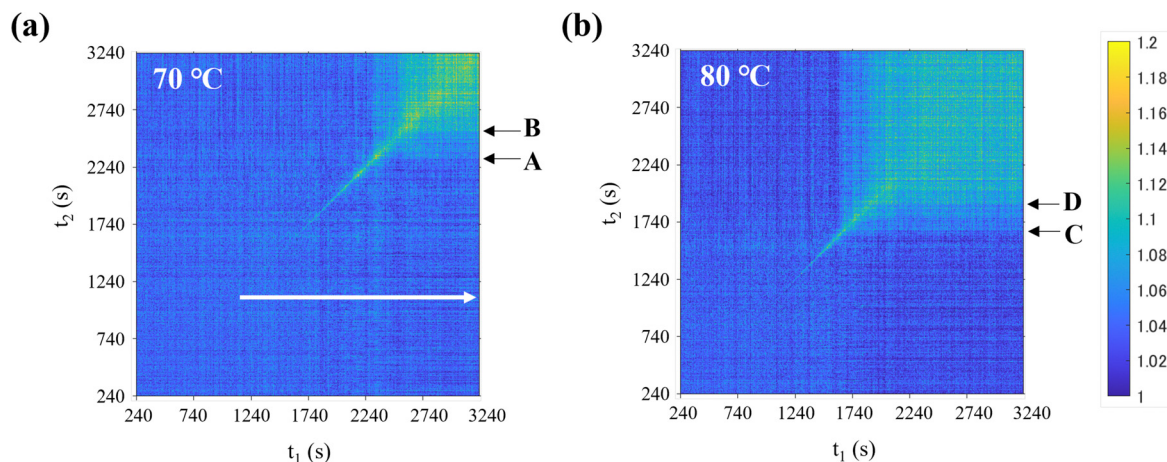
Fig. 2 Two-time correlation function C_I for $q_{\parallel} = 1.78 \times 10^{-3}$ nm^{-1} at 70 (a) and 80 °C (b). The correlation function at a specific time can be evaluated by cutting out horizontally as shown by the white arrow. Arrows A and B in (a) correspond to $t_w = 2320$ and 2540 s, respectively, and arrows C and D in (b) correspond to $t_w = 1620$ and 1890 s, respectively.
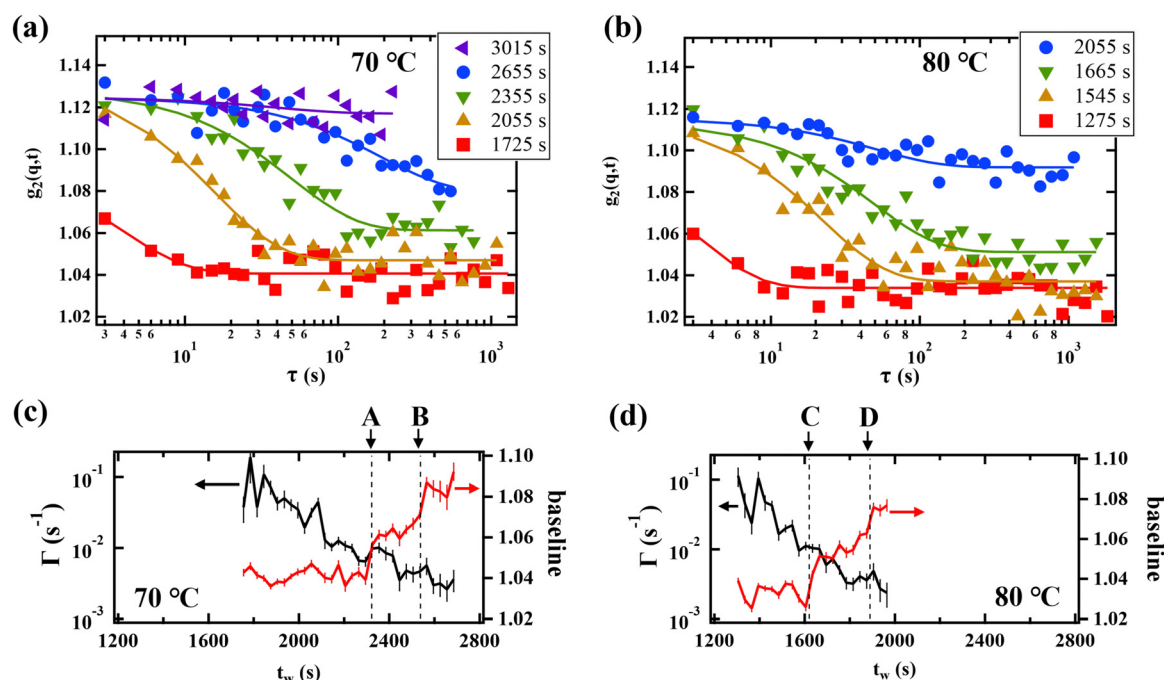

Fig. 3 g_2 at various time t_w cuts from C_I for $q_{\parallel} = 1.78 \times 10^{-3}$ nm^{-1} at 70 (a) and 80 °C (b). t_w dependence of Γ and A obtained by fitting analysis with eqn (2) at 70 (c) and 80 °C (d). The arrows A, B, C, and D correspond to those in Fig. 2.

At both temperatures, Γ decreases almost monotonically, which indicates that the surface fluctuations were slowing down due to the progress in the curing process. Moreover, baseline is almost constant at the beginning, but shows a sudden rise at $t_w \approx 2320$ s at 70 °C (corresponding to arrow A in Fig. 2a) and at $t_w \approx 1620$ s at 80 °C (corresponding to arrow C in Fig. 2b), followed by a gradual increase. The values of baseline larger than 1 suggest the presence of a relaxation slower than the measurement time. At 80 °C, the slight relaxation behaviour is observed in the slow time region (~ 1000 s) at

$t_w = 1275$ and 1545 s as shown in Fig. 3b. Although the detailed analysis was difficult because such data was rare and scattered, this might be a precursor to a subsequent rise in baseline. The rise of baseline indicates that the slow fluctuations became more pronounced relative to the fast relaxation corresponding to the first term of eqn (2). The physical discussion of the slow relaxation will be held later.

We first discuss the fast relaxation characterized by Γ in the first term of eqn (2). Fig. 4 shows Γ–q plots at various t_w. For highly viscous fluids, the capillary wave spectrum does not
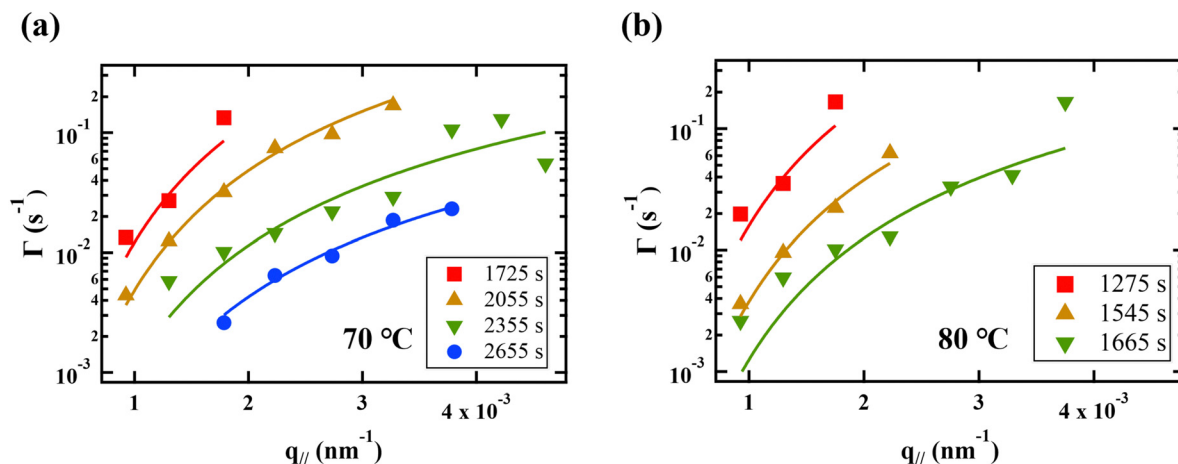
Fig. 4 $q_\parallel$ dependence of at various t_w at 70 (a) and 80 °C (b).

oscillate but shows an overdamped behaviour, which can be expressed by eqn (2).[26,36] Based on the hydrodynamic theory and fluctuation–dissipation theorem,[37–39] the $q_\parallel$ dependence of Γ in the overdamped regime on the surface of a viscous liquid polymer thin film with a nonslip boundary condition underneath is

$$\Gamma = \frac{\gamma}{2\eta}q_\parallel \frac{\sinh(q_\parallel d)\cosh(q_\parallel d) - q_\parallel d}{\cosh^2(q_\parallel d) + (q_\parallel d)^2} \qquad (3)$$

where γ, η, and d are the surface tension, viscosity, and film thickness, respectively. The solid line in Fig. 4 is the result of fitting the measured data with $\gamma/2\eta$ as a free parameter. All data are in good agreement, which indicates that the fast relaxation behaviour originates from capillary waves due to the viscous liquid behaviour of the thin film. The t_w dependence of $\gamma/2\eta$ at 70 and 80 °C, obtained from fitting with eqn (3), is shown in Fig. 5. At both temperatures, $\gamma/2\eta$ shows a clear decrease of 2 to 3 orders of magnitude. Considering that the change in the surface tension γ is small[40] and the viscosity of bulk diamine epoxy resins increases by three orders of magnitude[41] during the curing process, these $\gamma/2\eta$ behaviours are reasonable.

It should be informative to compare the mechanical properties obtained by the GI-XPCS measurements with those of the bulk system to evaluate the curing state. Fig. 6 shows the storage (G') and loss (G'') moduli obtained during the curing process in the bulk sample and the viscosity η estimated from Cox–Merz empirical relationship, $\eta = |G^*|/\omega$, where $G^* = G' + iG''$ and ω is the angular frequency. The values of η at $t_w = 2320$ s at 70 °C (arrow A) and $t_w = 1620$ s at 80 °C (arrow C) for the thin films are roughly estimated to be $\sim 5 \times 10^5$ Pa s and $\sim 3 \times 10^5$ Pa s, respectively, from Fig. 5 using $\gamma \approx 40$ mN m^{-1}. When these values are compared to the values of η in the bulk system in Fig. 6 (indicated by A′ and C′), and the epoxy resins of the thin films are assumed to be in the sufficiently progressed curing state.

Although the fast relaxation behaviour was well explained by the capillary waves for simple viscous liquids, the behaviour of baseline might be affected by complex phenomena. It has been
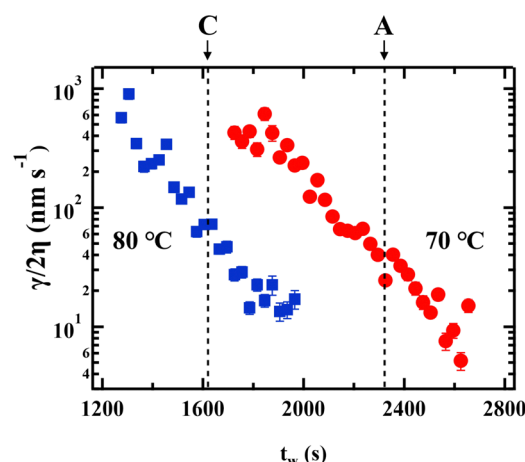

Fig. 5 t_w dependence of $\gamma/2\eta$ in the curing process at 70 and 80 °C. The arrows A and C correspond to those in Fig. 2.

reported that when the film thickness is sufficiently close to the radius of gyration of the molecule, the capillary wave exhibits viscoelastic behaviour.[42] In the curing process of diamine epoxy resins, oligomerization due to progressive chemical bonding at one end of DGEBA is thought to occur first, followed by gelation, in which oligomers (or polymers) cross-link each other due to chemical bonding at the opposite end, followed by densification of the cross-links. The increase in radius of gyration and the crosslink densification can cause the viscoelastic behaviour of the capillary waves. The rapid increases of baseline observed at arrows A and C in Fig. 2 indicate the development of additional slow kinetic mode, and they can be the expression of the viscoelastic behaviour. The film thickness dependence and reaction pathway dependence should provide important information. They should be subjects for future work.

After arrows B and D, all the measured surface fluctuations almost stopped in the measurement time range. This indicates that the gelation has been completed and the process of
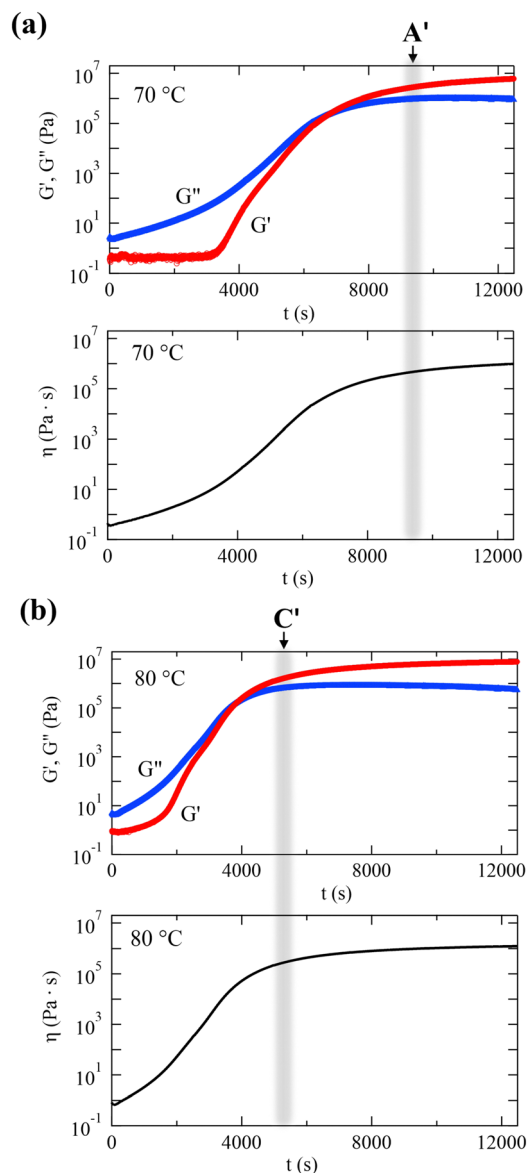
(a)

(b)

Fig. 6 Time dependence of the storage (G') and loss (G'') moduli obtained during the curing process in the bulk system (top) and the viscosity η estimated from Cox–Merz empirical relationship (bottom) at 70 (a) and 80 °C (b). The arrows A' and C' are around the corresponding value of η estimated for the thin films at A and C in Fig. 5, respectively.

crosslink densification has progressed. All the phenomena appeared at 80 °C earlier than at 70 °C, which is reasonable considering that curing proceeds faster at higher temperatures.

4 Conclusions

The surface dynamics in thin films of epoxy resin, with DGEBA as a base resin and DDM as a curing agent during the thermal curing process, were investigated using GI-XPCS. We measured the capillary wave spectra for the thin films during the thermal curing process and showed that these spectra, which slowed down with the reaction process, can be explained in the frame of the capillary wave theory for viscous liquids. In addition, a sudden rise and increase of baseline were observed at the later stage, which is assumed to be due to the gelation process. Finally, almost no relaxation behaviour was observed in the capillary wave spectra, indicating that the gelation was almost complete. In this study, we clearly showed that the freezing of the surface fluctuations of thermoset thin films are observable in a non-contact characterization, using the GI-XPCS technique. Compared to the bulk system, it has been difficult to know the thin film condition in a non-contact manner, but this approach allows to examine the curing condition as it is, which could be used to optimize the curing time and temperature in heating and the power in ultraviolet (UV) curing.

In the present study, the films were relatively thick, and the data could be analyzed without regard to heterogeneity within the film. Since the capillary waves in thin films with inhomogeneous viscosity behave differently from eqn (3), it is informative to collect and discuss the data at various thickness.[31,43] It should be also significant to distinguish between surface and internal dynamics by using a thin film with dispersed probe particles and tuning the incident angle.[44,45] Similar measurements can be performed under other conditions, such as ultraviolet light UV curing, and a deeper understanding of the curing mechanisms in various thin films is expected in the future.

Author contributions

T. H., Y. O., and A. Y. designed the research; T. H., Y. O., A. Y., and H. M. performed XPCS measurements. T. H. and Y. O. prepared the samples. T. H. analyzed the XPCS data. T. H., Y. O., and A. Y. interpreted the data. T. H. wrote the paper.

Conflicts of interest

There are no conflicts to declare.

Acknowledgements

Notes and references

1 J. P. Pascault and R. J. J. Williams, *Epoxy Polymers: New Materials and Innovations*, Wiley-VCH Verlag, 2010.
2 F.-L. Jin, X. Li and S.-J. Park, *J. Ind. Eng. Chem.*, 2015, **29**, 1–11.
3 R. B. Prime, Thermosets, in *Thermal Characterization of Polymeric Materials*, ed. E. A. Turi, Academic Press, San Diego, 1997, pp. 1379–1766.
4 R. Hardis, J. L. P. Jessop, F. E. Peters and M. R. Kessler, *Composites, Part A*, 2013, **49**, 100–108.

5 H. Ma, X. Zhang, F. Ju and S. B. Tsai, *Sci. Rep.*, 2018, **8**, 3045.

6 C. K. Tziamtzi and K. Chrissafis, *Polymer*, 2021, **230**, 124091.

7 P. Musto, M. Abbate, G. Ragosta and G. Scarinzi, *Polymer*, 2007, **48**, 3703–3716.

8 M. Aldridge, A. Wineman, A. Waas and J. Kieffer, *Macromolecules*, 2014, **47**, 8368–8376.

9 J. Mijovic and S. Andjelic, *Macromolecules*, 1995, **28**, 2787–2796.

10 J. P. Eloundou, M. Feve, J. F. Gerard, D. Harran and J. P. Pascault, *Macromolecules*, 1996, **29**, 6907–6916.

11 H. H. Winter and M. Mours, *Adv. Polym. Sci.*, 1997, **134**, 165–234.

12 D. J. O'Brien, P. T. Mather and S. R. White, *J. Compos. Mater.*, 2001, **35**, 883–904.

13 A. Bandyopadhyay, P. K. Valavala, T. C. Clancy, K. E. Wise and G. M. Odegard, *Polymer*, 2011, **52**, 2445–2452.

14 A. Shundo, M. Aoki, S. Yamamoto and K. Tanaka, *Macromolecules*, 2021, **54**, 9618–9624.

15 Y. Kawagoe, G. Kikugawa, K. Shirasu and T. Okabe, *Soft Matter*, 2021, **17**, 6707–6717.

16 B. M. Yavitt, D. Salatto, Z. Huang, Y. T. Koga, M. K. Endoh, L. Wiegart, S. Poeller, S. Petrash and T. Koga, *J. Appl. Phys.*, 2020, **127**, 114701.

17 T. Hoshino, Y. Okamoto, A. Yamamoto and H. Masunaga, *Sci. Rep.*, 2021, **11**, 9767.

18 E. B. Trigg, L. Wiegart, A. Fluerasu and H. Koerner, *Macromolecules*, 2021, **54**, 6575–6584.

19 C. H. Kim, D. Tondelier, B. Geffroy, Y. Bonnassieux and G. Horowitz, *Eur. Phys. J.: Appl. Phys.*, 2012, **57**, 20201.

20 E. Foo, M. Jaafar, A. Aziz and L. C. Sim, Properties of spin coated epoxy/silica thin film composites: Effect of nano- and micron-size fillers, *Composites, Part A*, 2011, **42**, 1432–1437.

21 Z. A. Ghaleb, M. Mariatti and Z. M. Ariff, *Composites, Part A*, 2014, **58**, 77–83.

22 A. A. Roche, J. Bouchet and S. Bentadjine, *Int. J. Adhes. Adhes.*, 2002, **22**, 431–441.

23 C. Wehlack and W. Possart, *Macromol. Symp.*, 2004, **205**, 251–262.

24 T. Hirai, K. Kawasaki and K. Tanaka, *Phys. Chem. Chem. Phys.*, 2012, **14**, 13532–13534.

25 K. Yamaguchi, D. Kawaguchi, N. Miyata, T. Miyazaki, H. Aoki, S. Yamamoto and K. Tanaka, *Phys. Chem. Chem. Phys.*, 2022, **24**, 21578–21582.

26 D. Langevin, *Light scattering by liquid surfaces and complementary techniques*, Surfactant science series, M. Dekker, New York, 1992, p. 41.

27 T. Hoshino, Y. Ohmasa, R. Osada and M. Yao, *Phys. Rev. E: Stat., Nonlinear, Soft Matter Phys.*, 2008, **78**, 061604.

28 R. Osada, T. Hoshino, K. Okada, Y. Ohmasa and M. Yao, *J. Chem. Phys.*, 2009, **130**, 184705.

29 Y. Ohmasa, T. Hoshino, R. Osada and M. Yao, *Phys. Rev. E: Stat., Nonlinear, Soft Matter Phys.*, 2009, **79**, 061601.

30 S. K. Sinha, Z. Jiang and L. B. Lurio, *Adv. Mater.*, 2014, **26**, 7764–7785.

31 T. Hoshino, S. Nojima, M. Sato, T. Hirai, Y. Higaki, S. Fujinami, D. Murakami, S. Ogawa, H. Jinnai, A. Takahara and M. Takata, *Polymer*, 2016, **105**, 487–499.

32 H. Masunaga, H. Ogawa, T. Takano, S. Sasaki, S. Goto, T. Tanaka, T. Seike, S. Takahashi, K. Takeshita and N. Nariyama, *et al.*, *Polym. J.*, 2011, **43**, 471–477.

33 G. Brown, P. A. Rikvold, M. Sutton and M. Grant, *Phys. Rev. E*, 1997, **56**, 6601–6612.

34 A. Malik, A. R. Sandy, L. B. Lurio, G. B. Stephenson, S. G. J. Mochrie, I. McNulty and M. Sutton, *Phys. Rev. Lett.*, 1998, **81**, 5832–5835.

35 O. Bikondoa, *J. Appl. Crystallogr.*, 2017, **50**, 357–368.

36 Y. Ohmasa, T. Hoshino, R. Osada and M. Yao, *Chem. Phys. Lett.*, 2008, **455**, 184–188.

37 J. L. Harden, H. Pleiner and P. A. Pincus, *J. Chem. Phys.*, 1991, **94**, 5208–5221.

38 J. Jäckle, *J. Phys.: Condens. Matter*, 1998, **10**, 7121–7131.

39 H. Kim, A. Rühm, L. B. Lurio, J. K. Basu, J. Lal, D. Lumma, S. G. J. Mochrie and S. K. Sinha, *Phys. Rev. Lett.*, 2003, **90**, 068302.

40 J. R. Abbott and B. G. Higgins, *J. Polym. Sci., Part A: Polym. Chem.*, 1988, **26**, 1985–1988.

41 M. Younes, S. Wartewig, D. Lellinger, B. Strehmel and V. Strehmel, *Polymer*, 1994, **35**, 5269–5278.

42 Z. Jiang, H. Kim, X. Jiao, H. Lee, Y. J. Lee, Y. Byun, S. Song, D. Eom, C. Li, M. H. Rafailovich, L. B. Lurio and S. K. Sinha, *Phys. Rev. Lett.*, 2007, **98**, 227801.

43 Z. Jiang, H. Kim, S. G. J. Mochrie, L. B. Lurio and S. K. Sinha, *Phys. Rev. E*, 2006, **74**, 011603.

44 S. Narayanan, D. R. Lee, A. Hagman, X. Li and J. Wang, *Phys. Rev. Lett.*, 2007, **98**, 185506.

45 T. Koga, C. Li, M. K. Endoh, J. Koo, M. Rafailovich, S. Narayanan, D. R. Lee, L. B. Lurio and S. K. Sinha, *Phys. Rev. Lett.*, 2010, **104**, 066101.